Research Article | Vol. 24, No. 22 | 31 Oct 2016 | OPTICS EXPRESS 25885

Optics EXPRESS

Novel aluminum plasmonic absorber enhanced by extraordinary optical transmission

QIANG LI,[1,2] ZIZHENG LI,[1] HAIGUI YANG,[1,*] HAI LIU,[1] XIAOYI WANG,[1] JINSONG GAO,[1,2,3] AND JINGLI ZHAO[1]

[1]*Key Laboratory of Optical System Advanced Manufacturing Technology, Changchun Institute of Optics, Fine Mechanics and Physics, Chinese Academy of Sciences, Changchun 130033, China*
[2]*University of the Chinese Academy of Sciences, Beijing 100039, China*
[3]*gaojs999@163.com*
[*]*yanghg@ciomp.ac.cn*

Abstract: We report a theoretical and experimental study on a novel type of aluminum super absorber which exhibits a near perfect absorption based on the surface plasmon resonance in the visible and near-infrared spectrum. The absorber consists of Ag/SiO_2/Al triple layers in which the top Al layer is patterned by a periodic nano hole array. The absorption spectrum can be easily controlled by adjusting the structure parameters including the radius of the nano hole and the maximal absorption can reach 99.0% in theory. We completely analyze the SPP and LSP modes supported by the metal-dielectric-metal structure and their contribution to the ultrahigh absorption. On this basis, we find a novel method to enhance the absorption via the simultaneous excitation of SPP at different interfaces theoretically and experimentally. Moreover, for the first time we clarify the EOT caused by the nano hole array can enhance the absorption by experiment, which is not reported in previous works. This kind of absorber can be fabricated by low-cost colloidal sphere lithography and the use of stable Al overcomes the disadvantages brought by the noble metal, which make it a more appropriate candidate for photovoltaics, spectroscopy, photodetectors, sensing, and surface enhanced Raman scattering.

OCIS codes: (240.6680) Surface plasmons; (310.6628) Subwavelength structures, nanostructures; (250.5403) Plasmonics.

References and links

1. C. M. Watts, X. Liu, and W. J. Padilla, "Metamaterial electromagnetic wave absorbers," Adv. Mater. **24**(23), OP98–OP120 (2012).
2. S. Y. Chou and W. Ding, "Ultrathin, high-efficiency, broad-band, omniacceptance, organic solar cells enhanced by plasmonic cavity with subwavelength hole array," Opt. Express **21**(S1), 60–76 (2013).
3. Y. H. Su, Y. F. Ke, S. L. Cai, and Q. Y. Yao, "Surface plasmon resonance of layer-by-layer gold nanoparticles induced photoelectric current in environmentally-friendly plasmon-sensitized solar cell," Light Sci. Appl. **1**(6), e14 (2012).
4. H. Chalabi, D. Schoen, and M. L. Brongersma, "Hot-electron photodetection with a plasmonic nanostripe antenna," Nano Lett. **14**(3), 1374–1380 (2014).
5. B. Park, S. H. Yun, C. Y. Cho, Y. C. Kim, J. C. Shin, H. G. Jeon, Y. H. Huh, I. Hwang, K. Y. Baik, Y. I. Lee, H. S. Uhm, G. S. Cho, and E. H. Choi, "Surface plasmon excitation in semitransparent inverted polymer photovoltaic devices and their applications as label-free optical sensors," Light Sci. Appl. **3**(12), e222 (2014).
6. C. Argyropoulos, K. Q. Le, N. Mattiucci, G. D'Aguanno, and A. Alu, "Broadband absorbers and selective emitters based on plasmonic Brewster metasurfaces," Phys. Rev. B **87**(20), 205112 (2013).
7. W. W. Salisbury, "Absorbent body for electromagnetic waves," U. S. patent 2599944 (June 10, 1952).
8. A. E. Cetin, D. Etezadi, B. C. Galarreta, M. P. Busson, Y. Eksioglu, and H. Altug, "Plasmonic nanohole arrays on a robust hybrid substrate for highly sensitive label-free biosensing," ACS Photonics **2**(8), 1167–1174 (2015).
9. C. Valsecchi and A. G. Brolo, "Periodic metallic nanostructures as plasmonic chemical sensors," Langmuir **29**(19), 5638–5649 (2013).
10. D. Z. Lin, Y. P. Chen, P. J. Jhuang, J. Y. Chu, J. T. Yeh, and J. K. Wang, "Optimizing electromagnetic enhancement of flexible nano-imprinted hexagonally patterned surface-enhanced Raman scattering substrates," Opt. Express **19**(5), 4337–4345 (2011).

#276068 http://dx.doi.org/10.1364/OE.24.025885
Journal © 2016 Received 20 Sep 2016; revised 23 Oct 2016; accepted 23 Oct 2016; published 28 Oct 2016

Optics EXPRESS

11. G. Dayal and S. A. Ramakrishna, "Design of highly absorbing metamaterials for infrared frequencies," Opt. Express **20**(16), 17503–17508 (2012).
12. J. Wang, C. Fan, P. Ding, J. He, Y. Cheng, W. Hu, G. Cai, E. Liang, and Q. Xue, "Tunable broad-band perfect absorber by exciting of multiple plasmon resonances at optical frequency," Opt. Express **20**(14), 14871–14878 (2012).
13. C. F. Guo, T. Y. Sun, F. Cao, Q. Liu, and Z. F. Ren, "Metallic nanostructures for light trapping in energy harvesting devices," Light Sci. Appl. **3**(4), e161 (2014).
14. Y. Chu, M. G. Banaee, and K. B. Crozier, "Double-resonance plasmon substrates for surface-enhanced Raman scattering with enhancement at excitation and stokes frequencies," ACS Nano **4**(5), 2804–2810 (2010).
15. G. Li, Y. Shen, G. Xiao, and C. Jin, "Double-layered metal grating for high-performance refractive index sensing," Opt. Express **23**(7), 8995–9003 (2015).
16. N. Papanikolaou, "Optical properties of metallic nanoparticle arrays on a thin metallic film," Phys. Rev. B **75**(23), 235426 (2007).
17. F. Cheng, X. Yang, D. Rosenmann, L. Stan, D. Czaplewski, and J. Gao, "Enhanced structural color generation in aluminum metamaterials coated with a thin polymer layer," Opt. Express **23**(19), 25329–25339 (2015).
18. F. Cheng, J. Gao, L. Stan, D. Rosenmann, D. Czaplewski, and X. Yang, "Aluminum plasmonic metamaterials for structural color printing," Opt. Express **23**(11), 14552–14560 (2015).
19. Z. Y. Fang, Y. R. Zhen, L. R. Fan, X. Zhu, and P. Nordlander, "Tunable wide-angle plasmonic perfect absorber at visible frequencies," Phys. Rev. B **85**(24), 245401 (2012).
20. J. M. Hao, J. Wang, X. L. Liu, W. J. Padilla, L. Zhou, and M. Qiu, "High performance optical absorber based on a plasmonic metamaterial," Appl. Phys. Lett. **96**(25), 251104 (2010).
21. T. W. Ebbesen, H. J. Lezec, H. F. Ghaemi, T. Thio, and P. A. Wolff, "Extraordinary optical transmission through sub-wavelength hole arrays," Nature **391**(6668), 667–669 (1998).
22. H. F. Ghaemi, T. Thio, D. E. Grupp, T. W. Ebbesen, and H. J. Lezec, "Surface plasmons enhance optical transmission through subwavelength holes," Phys. Rev. B **58**(11), 6779–6782 (1998).
23. W. Yue, Z. Wang, Y. Yang, J. Li, Y. Wu, L. Chen, B. Ooi, X. Wang, and X. X. Zhang, "Enhanced extraordinary optical transmission (EOT) through arrays of bridged nanohole pairs and their sensing applications," Nanoscale **6**(14), 7917–7923 (2014).
24. S. Shu and Y. Y. Li, "Triple-layer Fabry-Perot/SPP aluminum absorber in the visible and near-infrared region," Opt. Lett. **40**(6), 934–937 (2015).
25. J. Yu, Q. Yan, and D. Shen, "Co-self-assembly of binary colloidal crystals at the air-water interface," ACS Appl. Mater. Interfaces **2**(7), 1922–1926 (2010).
26. S. H. Lee, K. C. Bantz, N. C. Lindquist, S. H. Oh, and C. L. Haynes, "Self-assembled plasmonic nanohole arrays," Langmuir **25**(23), 13685–13693 (2009).
27. E. D. Palik, *Handbook of Optical Constants of Solids* (Academic Press, 1985).
28. C. Genet and T. W. Ebbesen, "Light in tiny holes," Nature **445**(7123), 39–46 (2007).

1. Introduction

Super absorber [1] has attracted much attention due to its greatly potential applications in solar cell [2,3], photo detectors [4], sensing [5], and thermal emitting [6]. The first absorber was created in 1952 for the military to absorb radar waves with a three-layer structure [7], but it was eliminated for its bulk thickness. Recently, surface plasmon resonance (SPR) around metallic nanostructures provides an unprecedented way to manipulate the interaction between the light and matter at nanoscale, which plays a vital role in various fields such as biological and chemical sensors [8,9], surface-enhanced Raman scattering (SERS) [10], and energy harvesting [11–13]. SPR is coherent oscillations of electrons at metal-dielectric interfaces that can be categorized into propagating surface plasmons (PSPs) and localized surface plasmons (LSPs) [14]. Absorbers based on SPR have been widely studied both theoretically and experimentally in arrays of metallic gratings [15], nanoparticles [16], nano hole array [17–19], and nano cube [20] in recent years due to their controllable and superior absorption properties in the visible and near-infrared by engineering the shape, size, material of the structure as well as its dielectric environment. However, these absorbers based on plasmonic nanostructures usually involve expensive, time-costly and high-resolution nano fabrication processing steps such as electron beam lithography (EBL) and focused ion beam (FIB) which turn out to be a challenge for the application in large area of these patterned absorber.

Extraordinary optical transmission (EOT) was first discovered by Ebbesen and associates in 1998 [21]. When incident light interacts with the subwavelength hole array patterned in the optical thick metal film, the transmission intensity can be several orders stronger than the prediction from classic Bethe theory. EOT has attracted much attention due to its fundamental

Optics EXPRESS

importance and many potential use, including chemical sensors and biosensors [8,9]. Although the origin of EOT is controversial now, it is generally accepted that the excitation of surface plasmon modes on both surfaces of the metal film and their coupling to each other underlie the physics of the extraordinary transmission phenomena [22,23]. Yangyang Li and associates first applied the EOT effect in the super absorber using a metal-dielectric-metal (MDM) structure [24]. However, they just give several numerical simulations, lacking of experimental support.

In this paper, we fabricate a triple MDM structure which consists of a periodic nano hole array patterned in a 100 nm Al layer spaced by a thin SiO_2 film from a continuous 150 nm Ag layer as Fig. 1(a) shows. In this structure, Ag is chosen for its low material absorption and high reflection in the entire visible and near-infrared wavelength ranges. The middle SiO_2 dielectric spacing layer functions as a bridge to couple the SPP on the two metal films. The use of stable Al can overcome the disadvantages such as the intrinsic interband transition below the wavelength of 500 nm and oxidization brought by noble metal Au or Ag. Using this MDM structure, we proposed a novel method to enhance the absorption via the simultaneous excitation of SPP at different interfaces theoretically and experimentally. Moreover, we first clarify that the EOT effect has an important role in the absorption mechanism by experiment. The nano hole array is fabricated by colloidal sphere lithography, which has been widely exploited in the fabrication of nano structures, possessing advantages of large area, low cost, and easy fabrication process.

2. Experiment design and fabrication

We use a self-assembled nanosphere lithography to fabricate the periodic nano hole arrays, which is an efficient and inexpensive method to fabricate a large-area periodic nanostructures. The procedure for the fabrication is shown in Fig. 1(a). 150 nm thick Ag film and 50 nm thick SiO_2 film were deposited on the quartz glass substrate respectively with electron beam vapor deposition. The 50 nm thick SiO_2 film was optimized using 3D finite-difference time-domain (FDTD) simulation in order to obtain high absorption. We purchased 500 nm diameter polystyrene (PS) colloidal spheres and a close packed PS nanosphere monolayer was prepared by the interface method as the description in the references [25,26]. In order to obtain the non-close packed 2D colloidal crystals, the size of the PS nanospheres was reduced by oxygen plasma using reactive ion etching (RIE) in a controlled manner, with 250 w power, 30 mTorr pressure, 10 sccm O_2 flow rate. Afterward, a 100 nm thick Al layer was deposited vertically on the non-close packed 2D PS nanosphere mask. Finally, we removed the PS nanospheres using ultrasonic cleaning in toluene solution for 10 minutes, leading to the formation of nanohole array in the top Al layer. The atomic force microscopy (AFM) picture for the nano hole array is shown in Fig. 1(b). The period (L), radius (r) and depth of the hole are 500 nm, 170 nm and 100 nm respectively. The perpendicularity of the nano hole is relatively well. In this fabrication process, the period can be adjusted by the size of the PS nanospheres; the diameter of the nano holes can be controlled by different etching time of the RIE procedure; the thickness of Al layer is determined by the deposition process. The experimental reflection is measured using a PerkinElmer spectrometer equipped with an integrating sphere.

Optics EXPRESS

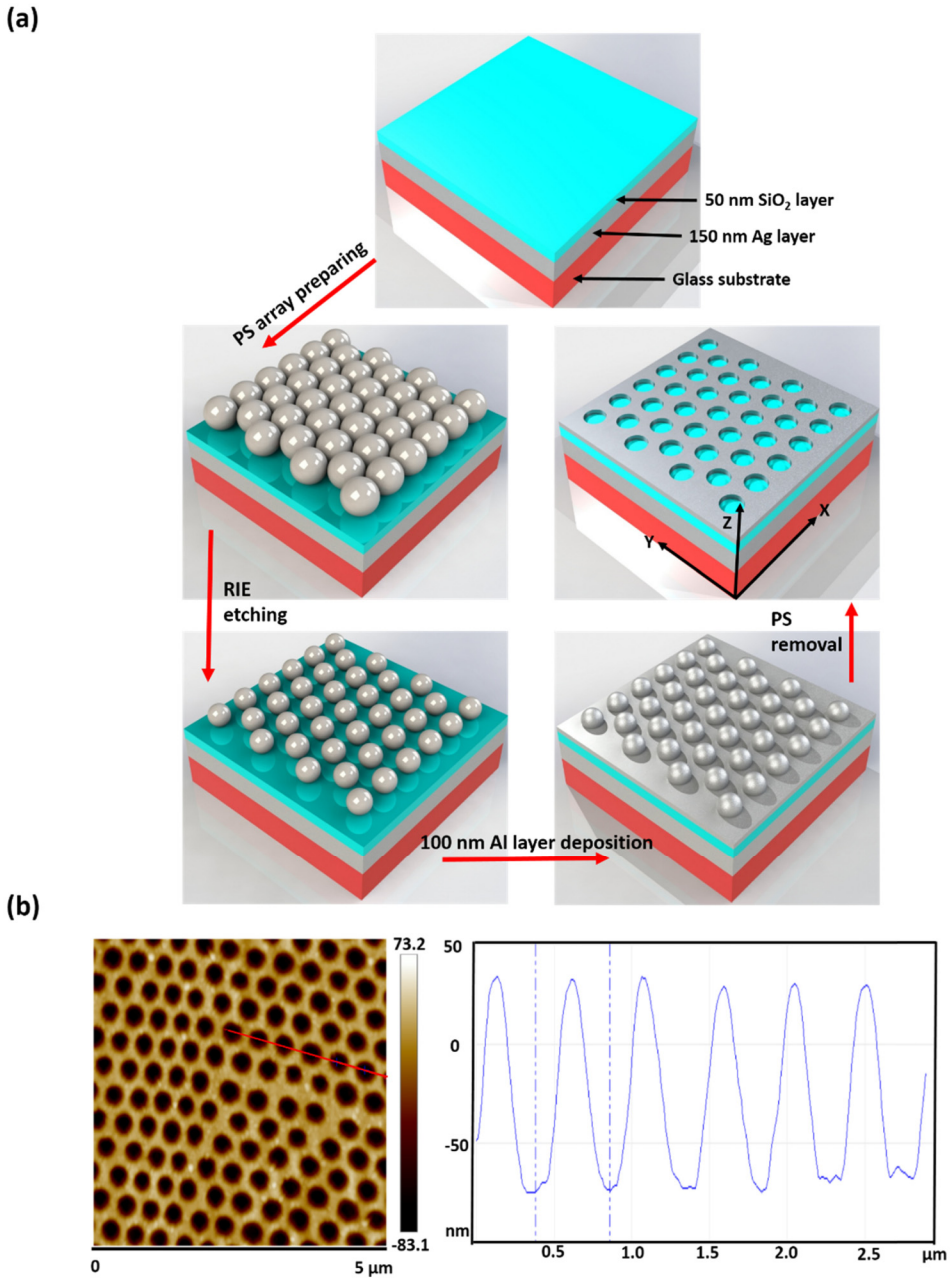

Fig. 1. (a) Fabrication process flow of the nano hole array in metal Al layer. (b) AFM image of fabricated 2D nano hole array, and surface fluctuation profile along the red line.

3. Numerical investigation

We perform the 3D finite-difference time-domain (FDTD) simulation to investigate the optical characteristic of the proposed absorber, where the periodic boundary conditions are used for a unit cell in the x-y plane and perfectly matched layers (PML) are applied in the z axis. A discrete mesh with the size of $2 \times 2 \times 1$ nm^3 is used for the Al layer. The permittivity of Ag, SiO_2, and Al used in simulation are extracted from the data of Palik [27]. The thickness of bottom Ag layer t is set to be 150 nm which is several times larger than the skin

Optics EXPRESS

depth so that the incident light transmission through the structure can be completely inhibited. Therefore, the absorption is $A = 1\text{-}R$ where R is the reflection. The incident light with a wavelength range from 400 nm to 1500 nm propagates along the negative z direction with the E field polarization in the x direction.

First of all, we investigate the MDM structure with nano hole array patterned on the top Al layer. We sweep the radius r of the nano hole with fixing period L = 500 nm and plot the simulated absorption as a function of r and the incident wavelength. It is evident from Fig. 2(a) that three different modes lead to three distinct absorption peaks marked as B_1, B_2, and B_3 in which the location of B_3 strongly depends on the radius r and B_1, B_2 almost stay constant with varying r. In according to previous work [14], the LSPs properties of metal nano structure mainly depend on its shape, size, material as well as the dielectric environment; for the SPP resonance frequency is determined by the array period and the angle of incident light. So in our situation, we attribute B_1, B_2 modes to the excitation of SPP by grating coupling, while B_3 mode is the LSPs around the nano hole. The black and white dash lines on the left indicating the wavelengths of 465.5 nm and 530.5 nm are in agreement with the B_1 and B_2 regions due to the (1,0) SPP propagating at the interfaces of Al/air and Ag/SiO_2 whose resonance wavelengths are determined by the following equations [28]:

$$k = k_0 \cdot \sin\theta + \sqrt{\frac{4}{3}\left(i^2 + i \cdot j + j^2\right)} \cdot \frac{2\pi}{L}. \tag{1}$$

$$k_{spp} = k_0 \cdot \sqrt{\frac{\varepsilon_m \cdot \varepsilon_d}{\varepsilon_m + \varepsilon_d}}. \tag{2}$$

Equation (1) is the Bragg coupling condition for the hexagonal arrays, in which $k_0 = \frac{w}{c}$ is the free-space wavevector, θ is the angle of the incident wave, i and j are the resonance orders, L is the period. Equation (2) indicates the wavevector of the SPP, ε_m and ε_d are the dielectric constant of metal and surrounding medium respectively. Only when $k = k_{spp}$ does the energy carried by the incident electromagnetic wave can be transferred to the SPP, which propagates along the interface of the metal and dielectric. For better understanding the physical origin of the absorption peaks B_1 and B_2, we calculate the relative magnetic field distributions on the x-z plane when radius r is 100 nm and period L is 500 nm. The simulated results are shown in Figs. 2(b) and 2(c). The magnetic field intensity is mainly confined at the interfaces of Air/Al and SiO_2/Ag, and the decay length into the metal is shorter than it in the dielectric medium, which indicate that the SPP mode is excited by the incident wave coupled with the nano hole array.

In order to clarify the role of EOT in the absorption mechanism, we investigate the EOT phenomenon of the 100 nm thick Al layer with nano hole array on the quartz glass substrate (n = 1.45). Here, we sweep the radius r of the nano hole with fixing period L = 500 nm and plot the simulated transmission as a function of r and the wavelength of the incident wave. As we can see from Fig. 2(d) that two transmission peaks stay constant with varying r, due to the fact EOT occurs when the SPP modes are excited and the resonance wavelength of SPP is independent of the value of r. The black dash lines show the SPP resonance wavelengths calculated by Eq. (1) and Eq. (2). The two different transmission peaks T_1 and T_2 can be assigned as the (1,0) SPP modes at the Al/air and Al/glass interfaces, which appear at 465.5 nm and 661.2 nm, respectively. The relative magnetic field distributions at the two transmission peak wavelengths are simulated on the x-z plane when r is 130 nm and L is 500 nm. As the Figs. 2(e) and 2(f) show, the magnetic field intensity is mainly confined at the Al/air and Al/glass interfaces, which are consistent with the calculated results and indicate that the SPP mode is excited.

Optics EXPRESS

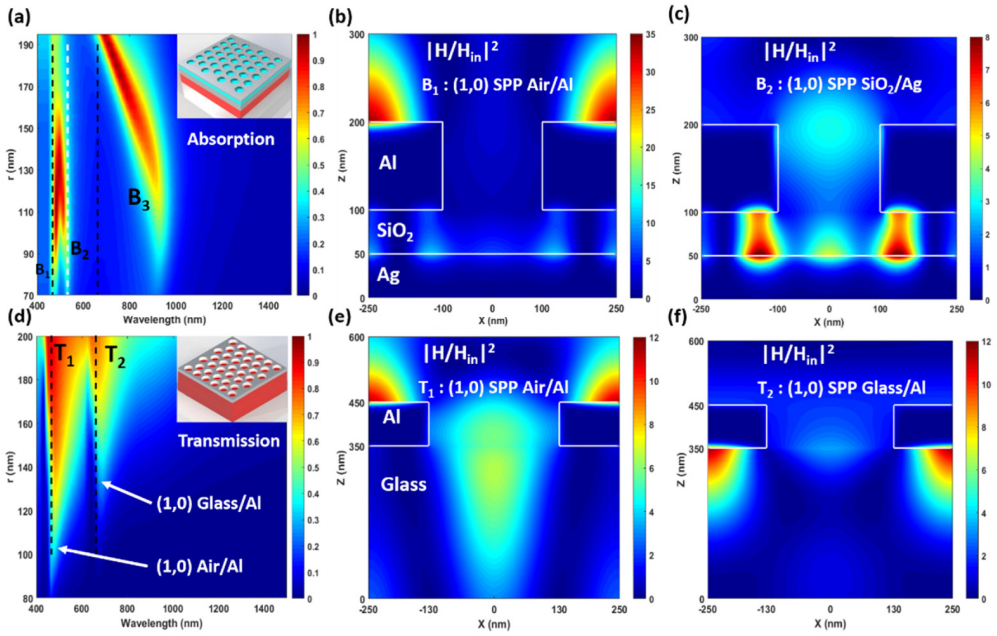

Fig. 2. (a) Absorption for the MDM absorber as a function of wavelength and the radius of the hole r with period L = 500 nm. The three dash lines represent the calculated positions of SPP using Eq. (1) and Eq. (2) in theory, in which from left to right are the (1,0) SPP at Al/air, Ag/SiO_2, and Al/SiO_2 interfaces, respectively. (b) and (c) The relative magnetic field distributions at the wavelength of peaks B_1 and B_2 on the x-z plane when r is 100 nm and period L is 500 nm. (d) Transmission as a function of wavelength and the radius r with period L is 500 nm for a 100 thick Al layer with nano hole array coated on the quartz glass. The black lines indicate the calculated positions of SPP using Eq. (1) and Eq. (2). (e) and (f) The relative magnetic field intensity distributions on the x-z plane at two transmission peak T_1 and T_2 for r = 130 nm and L = 500 nm.

The MDM absorber we proposed includes a top 100 nm thick Al film with nano hole array and a 50 nm SiO_2 film similar to the structure supporting EOT in Fig. 2(d), which indicates that the EOT phenomenon may play a part in the absorption mechanism. Many previous works have demonstrated that the SPP mode can enhance optical transmission [21–23]. We also confirm that the EOT phenomenon exists in the triple-layer absorber in the above section. So the nano hole array in the top Al layer enables enhanced light transmission through the SPP mode, and the light transmitted through the holes enters into the middle SiO_2 layer, and finally the energy gets absorbed at the interfaces of Al/SiO_2 and Ag/SiO_2, which is exactly as the description in the reference [24].

By contrasting Figs. 2(a) and 2(d), we can find two interesting phenomena: firstly, the absorption peak B_1 and the transmission peak T_1 are at the same wavelength because of the common origin of the excitation of (1,0) SPP at the Al/air interface. When the radius r is increasing, the (1,0) SPP at Al/air (B_1) and SiO_2/Ag (B_2) interfaces couple with each other leading to a hybrid mode which makes a contribution to a higher absorption. And the location of the hybrid mode is between the resonance wavelength of the (1,0) Al/air and (1,0) SiO_2/Ag. Figure 3(a) shows the calculated the relative magnetic field distributions on the x-z plane when r is 130 nm at the wavelength of the hybrid mode. The SPP is excited at the Al/air interface, and then enters the cavity, finally couples to the SPP at bottom Ag/SiO_2 interface across the SiO_2 layer. This process can be enhanced by the EOT effect, leading to more incident light couples to the SPP mode at bottom Ag/SiO_2 interface and then is consumed up there. When the value of r is further increasing, although the transmission intensity is

Optics EXPRESS

stronger, the absorption reduces because the top Al film turns into an uncontinuous state relative to the short wavelength, which limits the excitation of SPP mode.

Secondly, the absorption peak B_3 is abnormal blue shifted as the increasing value of r. This is because the size of metal Al structure is shrinking if r is enlarged. As mentioned above, the absorption peak B_3 is the result of excitation of LSPs, so the relative magnetic field distributions in Fig. 3(b) shows that the magnetic field is localized strongly in the SiO_2 spacing layer, which is clearly different from Fig. 3(a) and confirms the localized nature of the mode. In addition, the B_3 absorption intensity becomes stronger when its location is closer to the transmission peak T_2, which shows that more incident light passing through the nano hole array enhanced by the SPP can be localized in the SiO_2 spacing layer and is consumed by the metal Ag and Al. The plot of Poynting vector S (red arrows) in Figs. 3(c) and 3(d) vividly describe how the incident light propagates in the MDM structure. At first, the incident energy propagates along z-axis, and then enters the cavity through the nano hole. The difference occurs after the light enters into the SiO_2 spacing layer. In Fig. 3(c) the energy is running in parallel with the Ag/SiO_2 interface. While in Fig. 3(d) the energy whirls and converges under the Al film forming one magnetic dipole resonance.

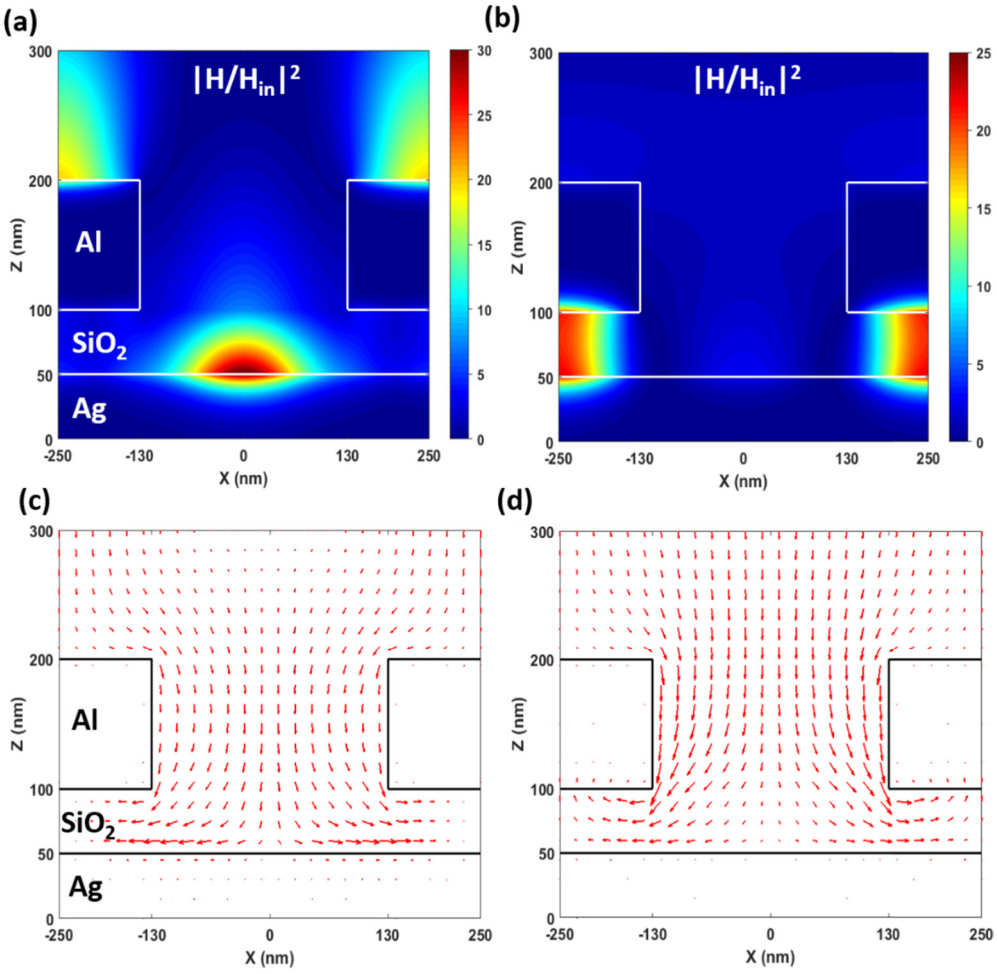

Fig. 3. The period and radius of the hole are L = 500 nm, r = 130 nm for the MDM absorber. (a) and (c) The relative magnetic field intensity distributions and the flow of Poynting vector at the wavelength of the hybrid mode. (b) and (d) The relative magnetic field intensity distributions and the flow of Poynting vector at the absorption peak B_3.

Optics EXPRESS

4. Experiment results and discussion

In order to fabricate the triple-layer absorber and verify the opinions we obtained from numerical simulation, we applied the self-assembled nanosphere lithography to fabricate the periodic hole arrays in the Al layer as Fig. 1(a) shows. Figures 4(a)-4(c) show the top-view scanning electron microscopy (SEM) images of three selected samples with the same period (500 nm) and different hole radius (100 nm, 130 nm and 170 nm), along with a magnified view of an individual nano hole in Fig. 4(b).

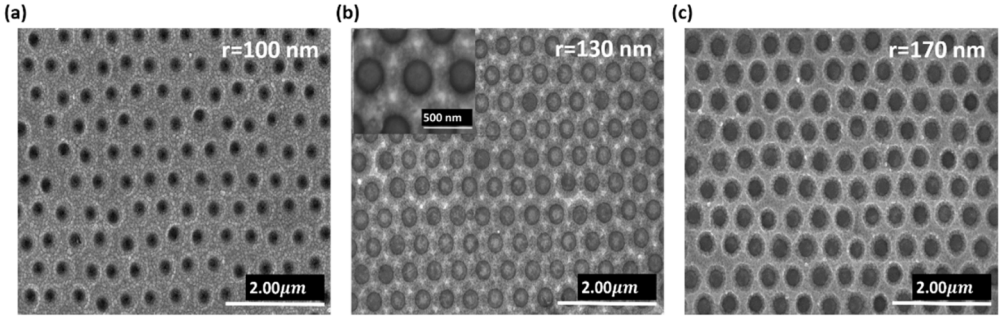

Fig. 4. (a), (b) and (c) The top view of three selected samples with same period 500 nm and different radius r = 100 nm, 130 nm and 170 nm. The magnified view of an individual nano hole is also shown in (b).

The experimental transmission and absorption are shown in Figs. 5(a) and 5(c) contrasted to the simulated results in Figs. 5(b) and 5(d). As we can see, the experimental absorption peak B_2 in infrared region is blue shifted when r is increasing from 100 nm to 170 nm. The absorption is stronger as the peak shifting to the resonance wavelength of the SPP (l,0) at the Al/SiO_2 interface indicating the EOT peak T_2, which shows that the EOT effect can play a positive role in the absorption mechanism. To the best of our knowledge, this is the first report to prove that the EOT caused by SPP can play an auxo-action in a such kind of absorber by experiment, which is completely different from the many previous absorbers in working mechanism. While for the absorption peak B_1, the locations of peaks are in accord with the transmission peak T_1 assigned as the (1,0) SPP at the Al/air interface. When r is 100 nm, there are two absorption peaks at the wavelengths of 548 nm and 660 nm which are attributed to the SPP at the Al/air and Ag/SiO_2 interfaces, respectively. Increasing r to the value of 130 nm, the two absorption peaks overlap with each other, forming one single absorption peak at the common resonance wavelength of 582 nm, which makes a contribution to an ultrahigh absorption 90%. This experimental results proves that the excitation of SPP at different interfaces simultaneously can enhance the absorption. It should be noted that the experimental results have some deviation from the simulation, which maybe originate from the fact that the shape of the nano hole fabricated by the self-assembled nanosphere lithography method is not a standard cylinder structure used in the simulation.

Optics EXPRESS

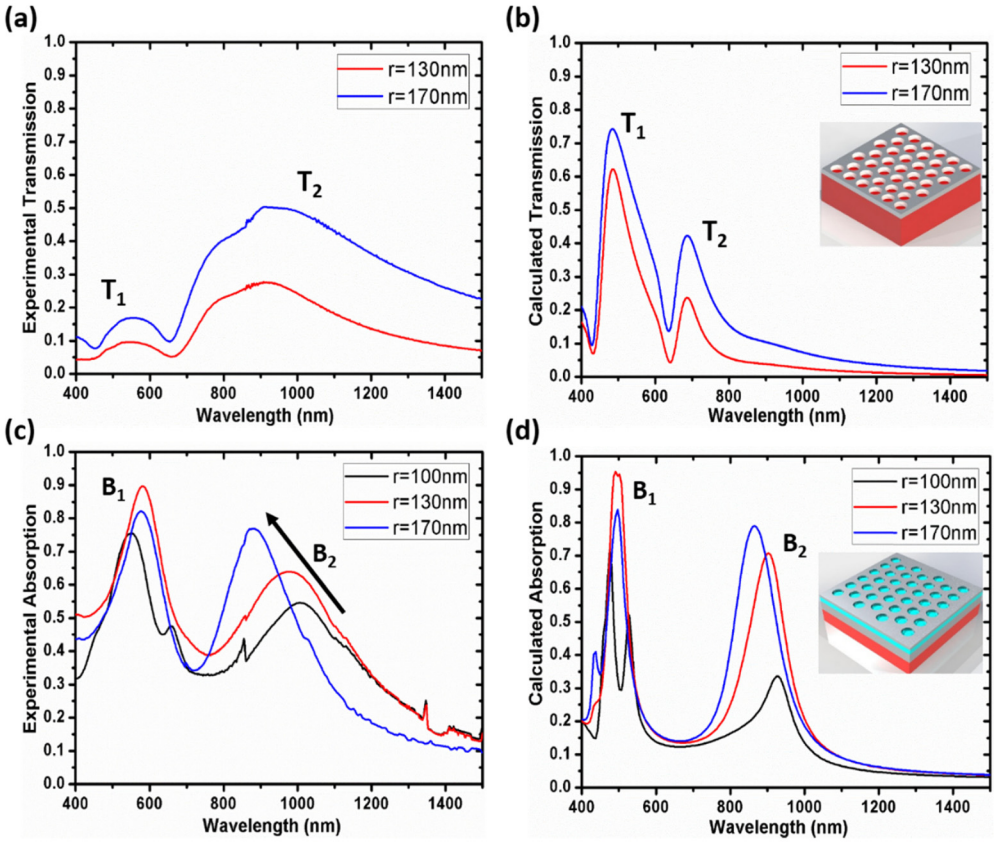

Fig. 5. (a) and (b) Experimental and simulated transmission of 100 nm thick Al layer with nano hole array coated on quartz glass substrate. The period L is 500 nm and radius r are 130 nm, 170 nm respectively. (c) and (d) Experimental and simulated absorption for MDM structure with the same period L = 500 nm, different r = 100 nm, 130 nm and 170 nm.

5. Conclusion

To summarize, we have successfully demonstrated a MDM super absorber based on surface plasmon resonance in the visible and infrared spectrum. We thoroughly analyzed the SPP and LSPs modes supported by the MDM structure and their relationship with the ultrahigh absorption. A novel method to further enhance the absorption via the simultaneous excitation of SPP at different interfaces is theoretically and experimentally studied, which is different from previous works. Moreover, we clarify experimentally that EOT caused by SPP plays a positive role in the absorption mechanism for the first time which provides a new perspective in designing this kind of super absorber. The absorber we proposed can be fabricated by a low-cost colloidal lithography, which make this kind of novel absorber to be a more appropriate candidate for photovoltaics, spectroscopy, sensing, photodetectors, and surface enhanced Raman scattering.

Funding

National Natural Science Foundation of China (NSFC) (Nos. U1435210, 61306125, 61675199 and 11604329); Science and Technology Innovation Project (Y3CX1SS143) of CIOMP; Science and Technology Innovation Project of Jilin Province (Nos. 20130522147JH and 20140101176JC).